Interaction and Multiscale Mechanics, Vol. 2, No. 1 (2009) 91-107
DOI: http://dx.doi.org/10.12989/imm.2009.2.1.091

A study on nonlinear seismic response analysis of building considering frequency dependent soil impedance in time domain

Naohiro Nakamura*

R&D Institute, Takenaka Corporation, 1-5-1, Ohtsuka, Inzai, Chiba, 270-1395, Japan

(Received March 23, 2008, Accepted August 15, 2008)

Abstract. In order to accurately estimate the seismic behavior of buildings, it is important to consider both nonlinear characteristics of the buildings and the frequency dependency of the soil impedance. Therefore, transform methods of the soil impedance in the frequency domain to the impulse response in the time domain are needed because the nonlinear analysis can not be carried out in the frequency domain. The author has proposed practical transform methods. In this paper, seismic response analyses considering frequency dependent soil impedance in the time domain are shown. First, the formulation of the proposed transform methods is described. Then, the linear and nonlinear earthquake response analyses of a building on 2-layered soil were carried out using the transformed impulse responses. Through these analyses, the validity and efficiency of the methods were confirmed.

Keywords: frequency dependency; time domain; earthquake response; soil impedance; impulse response.

1. Introduction

During severe earthquakes, buildings show nonlinear response behavior. It is also well known that the frequent dependency of the dynamic soil-structure interaction affects the response of buildings. Then, in order to accurately estimate the seismic behavior of buildings, both nonlinear characteristics of the buildings and the frequency dependency of the soil impedance should be considered. The nonlinear analysis can be carried out in the time domain while it cannot be done in the frequency domain. Therefore, transform methods of the soil impedance in the frequency domain to the impulse response in the time domain are needed.

When the frequency dependency of the soil impedance is weak, it can easily and accurately be transformed to the time domain using the Voigt model. However, the actual impedance often shows strong frequency dependency due to layers and inhomogeneity within the soil. Therefore, an accurate transform is often difficult.

Investigations into the transform to the time domain have been actively carried out for the past 2 decades. Wolf *et al*. (1985) proposed a method for performing response analyses in the time domain by using the impulse response obtained from the inverse Fourier transform of the soil impedance.

* E-mail: nakamura.naohiro@takenaka.co.jp

Hayashi *et al*. (1990) investigated the formulation of the transform method using the fast Fourier transform with consideration to the causality condition.

Besides, the recursive formula of the convolution integral from the soil impedance (e.g. Wolf *et al*. 1989, Meek 1990, Motosaka *et al*. 1992) and the methods using the lumped parameter models to approximate the soil impedance have also been studied for the same purpose (e.g. de Barros *et al*. 1990, Wolf 1997, Wu *et al*. 2002).

Although there were certain results from these studies, few cases are applied to the practical problems at present.

The author has proposed practical transform methods (Nakamura 2006a, 2006b). The impulse response of these methods is formulated considering the terms concerned with both the past displacement and velocity, while most of the previous methods employed either the past displacement or the past velocity.

In this paper, linear and nonlinear seismic response analyses of a building considering the frequency dependent soil impedance in the time domain are carried out. Especially, the efficiency of the proposed methods for the nonlinear analyses is studied for the first time.

First, the formulation of the proposed transform methods (Nakamura 2006b) is described. Method A is a basic method, and method B is a modified one for improving the accuracy by adding a virtual mass. Method C is modified further to deal with the large hysteretic damping. The soil impedances of 2-layered soil are computed using the thin layer element method (hereafter TLEM) (Tajimi 1980) and these soil impedances are transformed into the time domain using the proposed methods.

Next, linear earthquake response analyses of the structure on the 2-layered soil are carried out using the proposed method in the time domain. The validity of these analyses is confirmed by the comparison with the result of frequency response analyses and the conventional Voigt model.

Then, nonlinear earthquake response analyses using the proposed method are also performed in order to confirm the efficiency of the method.

Although the "impulse response" is often used as the transformed value to the time domain from both the impedance and the compliance functions, it always indicates the value from the impedance functions if there is no remark hereafter.

2. Transform method

The transform methods of frequency dependent soil impedance to the time domain utilized in this paper are as follows.

2.1 Basic method (Method A)

Although many methods to transform frequency dependent impedance to the time domain have been proposed, most of them employ either the past displacement or the past velocity in the formulation of the impulse response. On the contrary, the author proposed a transform method using both the past displacement and velocity (Nakamura 2006a).

Table 1 shows the components of the impulse response corresponding to those of the impedance. In the previous method, the simultaneous components (values concerning the current condition) and the time-delay components (values concerning the past condition) are considered. It is known that

Table 1 Considered components of impulse response with corresponding components of the complex stiffness

Components of impulse response	Simultaneous components ($t = 0$)	Time-delay components ($t > 0$)
Stiffness terms	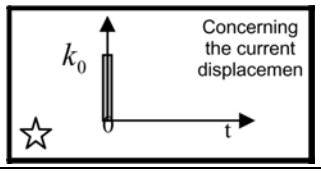	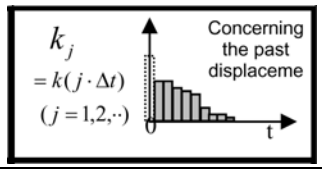
Damping terms	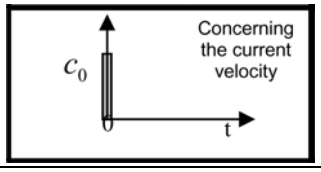	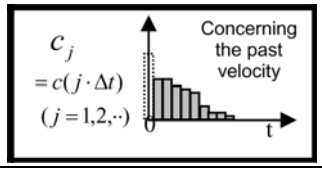
Mass terms	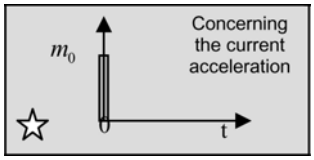	-
Corresponding components of impedance (in freq. domain)	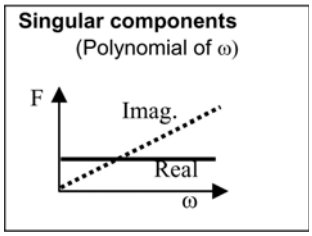	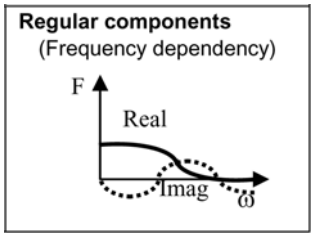

*1) ▭ Used components in method A
*2) ▭ Added component in method B
*3) ☆ Modified components in method C

the frequency dependency of the impedance is caused by the latter components. Both terms concerned with the displacement (hereafter referred to as the stiffness term) and the velocity (hereafter referred to as the damping term) are taken into account in the formulation.

Hereafter, the method is referred to as "method A". The complex stiffness and the reaction of method A are expressed in Eqs. (1) and (2), respectively. Where $u(t)$ is the displacement and is the velocity. $t_j = j\Delta t$ where Δt is the discrete time interval. c_j ($= c(t_j)$) and k_j ($= k(t_j)$) are the damping term and the stiffness term of the obtained impulse response function at t_j respectively. c_0 and k_0 are the simultaneous components and $c_1 \sim c_{N-1}$ and $k_1 \sim k_{N-1}$ are the time-delay components of each term.

$$S_A(\omega) = i\omega \cdot c_0 + k_0 + \left\{ i\omega \cdot \sum_{j=1}^{N-1} c_j \cdot e^{-i\omega t_j} + \sum_{j=1}^{N-1} k_j \cdot e^{-i\omega t_j} \right\} \tag{1}$$

$$F_A(t) = c_0 \cdot \dot{u}(t) + k_0 \cdot u(t) + \left\{ \sum_{j=1}^{N-1} c_j \cdot \dot{u}(t - t_j) + \sum_{j=1}^{N-1} k_j \cdot u(t - t_j) \right\} \tag{2}$$

Eq. (1) can be written as Eq. (3). By regarding $\{S_A(\omega_i)\}$ as the given impedance data $\{D(\omega_i)\}$, Eq. (3) can be rewritten as Eq. (4). This equation shows the relationship between the given impedance data $\{D(\omega_i)\}$ ($i = 0, 1, 2 \ldots N$) and the unknown impulse response components $\{G_{Ka}\}$ and $\{G_{Ca}\}$ as a form of simultaneous linear equations with the coefficient matrix $[[\overline{C}_{Ka}][\overline{C}_{Ca}]]$. The size of the coefficient matrix is $2N \times 2N$ because both $[\overline{C}_{Ka}]$ and $[\overline{C}_{Ca}]$ are $2N \times N$. The components of each vector and matrix are showed in Eq. (5) where $\theta_{ij} = \omega_j t_j$. The impulse response components can be obtained by solving this equation. This method can also be considered to be a special sort of a smooth interpolation between the given frequency data points which is always causal in the time domain.

$$\{S_A(\omega_i)\} = \begin{Bmatrix} \mathrm{Re}[S_A(\omega_i)] \\ \mathrm{Im}[S_A(\omega_i)] \end{Bmatrix} = \begin{Bmatrix} \sum_{j=0}^{N-1} \cos\theta_{ij} \cdot k_j + \omega_i \sum_{j=0}^{N-1} \sin\theta_{ij} \cdot c_j \\ -\sum_{j=0}^{N-1} \sin\theta_{ij} \cdot k_j + \omega_i \sum_{j=0}^{N-1} \cos\theta_{ij} \cdot c_j \end{Bmatrix} \tag{3}$$

$$\begin{Bmatrix} \{D(\omega_1)\} \\ \vdots \\ \{D(\omega_N)\} \end{Bmatrix} = [[\overline{C}_{Ka}][\overline{C}_{Ca}]] \cdot \begin{Bmatrix} \{G_{Ka}\} \\ \{G_{Ca}\} \end{Bmatrix} \tag{4}$$

where

$$\left.\begin{aligned} \{D(\omega_i)\} &= \begin{Bmatrix} \mathrm{Re}[D(\omega_i)] \\ \mathrm{Im}[D(\omega_i)] \end{Bmatrix}, \qquad \{G_{Ka}\} = \begin{Bmatrix} k_0 \\ k_1 \\ \vdots \\ k_{N-1} \end{Bmatrix}, \qquad \{G_{Ca}\} = \begin{Bmatrix} c_0 \\ c_1 \\ \vdots \\ c_{N-1} \end{Bmatrix} \\ [\overline{C}_{Ka}] &= \begin{bmatrix} \{\bar{c}_{K_{1,0}}\} & \cdots & \{\bar{c}_{K_{1,N-1}}\} \\ \vdots & \ddots & \vdots \\ \{\bar{c}_{K_{N,0}}\} & \cdots & \{\bar{c}_{K_{N,N-1}}\} \end{bmatrix}, \qquad \{\bar{c}_{K_{i,j}}\} = \begin{Bmatrix} \cos\theta_{ij} \\ -\sin\theta_{ij} \end{Bmatrix} \\ [\overline{C}_{Ka}] &= \begin{bmatrix} \{\bar{c}_{C_{1,0}}\} & \cdots & \{\bar{c}_{C_{1,N-1}}\} \\ \vdots & \ddots & \vdots \\ \{\bar{c}_{C_{N,0}}\} & \cdots & \{\bar{c}_{C_{N,N-1}}\} \end{bmatrix}, \qquad \{\bar{c}_{C_{i,j}}\} = \begin{Bmatrix} \omega_i \cdot \sin\theta_{ij} \\ \omega_i \cdot \cos\theta_{ij} \end{Bmatrix} \end{aligned}\right\} \tag{5}$$

2.2 Method with mass terms to improve the accuracy (Method B)

In order to improve the accuracy of the transform, a method is proposed in which the mass terms are considered only in the simultaneous component as shown in Eqs. (6) and (7) (Nakamura 2006b).

Hereafter, this method is called method B (See Table 1). It means that the virtual mass is considered in the estimation of the real part of the complex stiffness. With a view to balancing the number of unknowns and equations, $c_1 \sim c_{N\text{-}1}$ in method A are changed to $c_1 \sim c_{N\text{-}2}$.

$$S_B(\omega) = -\omega^2 \cdot m_0 + i\omega \cdot c_0 + k_0 + \left\{ i\omega \cdot \sum_{j=1}^{N-2} c_j \cdot e^{-i\omega t_j} + \sum_{j=1}^{N-1} k_j \cdot e^{-i\omega t_j} \right\} \tag{6}$$

$$F_B(t) = m_0 \cdot \ddot{u}(t) + c_0 \cdot \dot{u}(t) + k_0 \cdot u(t) + \left\{ \sum_{j=1}^{N-2} c_j \cdot \dot{u}(t-t_j) + \sum_{j=1}^{N-1} k_j \cdot u(t-t_j) \right\} \tag{7}$$

Eq. (3) can be rewritten as Eq. (8). So, the simultaneous equations can be set in the same way as Eqs. (4) and (5).

$$\{S_B(\omega_i)\} = \begin{Bmatrix} \mathrm{Re}[S_B(\omega_i)] \\ \mathrm{Im}[S_B(\omega_i)] \end{Bmatrix} = \begin{Bmatrix} \sum_{j=0}^{N-1} \cos\theta_{ij} \cdot k_j + \omega_i \sum_{j=0}^{N-2} \sin\theta_{ij} \cdot c_j - \omega_i^2 m_0 \\ -\sum_{j=0}^{N-1} \sin\theta_{ij} \cdot k_j + \omega_i \sum_{j=0}^{N-2} \cos\theta_{ij} \cdot c_j \end{Bmatrix} \tag{8}$$

In the case of part of the time delay components 1~n' being used, the complex stiffness and the reaction can be formulated as Eqs. (9) and (10) (under the condition of $n' < N$-1). The original data of the complex stiffness $D(\omega_i)$ is indicated as $D(\omega_i) = S_B(\omega_i)$ for $S_B(\omega_i)$ in Eq. (6), but $D(\omega_i) \neq S'_B(\omega_i)$ for $S'_B(\omega_i)$ in Eq. (9). The accuracy of the transform is improved very well by this modification especially in the case where the difference of the real part data of the given impedance between the minimum and maximum frequencies (Re $(D(\omega_1))$ and Re $(D(\omega_N))$) is large (see Nakamura 2006b).

$$S'_B(\omega) = -\omega^2 \cdot m_0 + i\omega \cdot c_0 + k_0 + \left\{ i\omega \cdot \sum_{j=1}^{n'} c_j \cdot e^{-i\omega t_j} + \sum_{j=1}^{n'} k_j \cdot e^{-i\omega t_j} \right\} \tag{9}$$

$$F'_B(t) = m_0 \cdot \ddot{u}(t) + c_0 \cdot \dot{u}(t) + k_0 \cdot u(t) + \left\{ \sum_{j=1}^{n'} c_j \cdot \dot{u}(t-t_j) + \sum_{j=1}^{n'} k_j \cdot u(t-t_j) \right\} \tag{10}$$

2.3 Method to improve for large damping (Method C)

In the case of the hysteretic damping being large, the accuracy of the recovered value in the real part of the impedance tends to deteriorate. In order to improve this tendency, the difference at all data points between the stiffness term and the mass term (m_0 and k_0) for the simultaneous component affecting only the real part as the subject to be corrected among the constitution components of the impulse response is minimized using the least square method (Ohsaki *et al.* 1978).

Hereafter, this method is called method C (See Table 1). The simultaneous components of the stiffness term and the mass term for the modified impulse response are set to be $k'_0 = k_0 + \Delta k$ and

$m'_0 + \Delta m$. Where, Δk and Δm indicate the modification terms. The recovered value of the complex stiffness can be expressed using Eq. (11).

$$S'_C(\omega) = S'_B(\omega) - \omega^2 \cdot \Delta m + \Delta k \tag{11}$$

From above, Method B is recommended for almost causal problems and Method C is recommended for all problems including non-causal problems, in general.

3. Seismic response of structure on 2-layered soil

In order to confirm the efficiency of the transform method, its applicability to the seismic response of the structure on the layered soil is investigated.

3.1 Analysis model

A five-storied reinforced concrete building shown in Fig. 1 with a base of 30 × 30 m on the 2-layered soil is analyzed.

The property of the base rock is linear with $Vs_2 = 500$ m/s. The surface layer is clay. Studies are carried out in two cases: where the property of the surface layer is linear (hereafter Soil-L) or nonlinear (hereafter Soil-NL).

For Soil-L, $Vs_1 = 200$ m/s and $h_1 = 2\%$ are used for the surface layer. For Soil-NL, the nonlinear dynamic soil characteristics (Ohsaki *et al*. 1978) shown in Fig. 2 are used. In order to use the Ramberg-Osgood model (hereafter R-O model), the soil characteristics are approximated as $\gamma = 0.1\%$ when $G/G_0 = 0.5$ and $h_{max} = 26\%$. The approximated characteristics correspond fairly well to the original Ohsaki's data as shown in Fig. 2.

The building is a multiple mass system model made by joining masses with shear springs. The soil-structure interaction is estimated by SR (sway and rocking) springs at the bottom of the basemat. The specifications of the building model are indicated in Table 2. The material damping ratio of the building is set at 0% in order to clearly show the effects of the estimation method of the dynamic soil stiffness.

3.2 Soil response analysis

First, soil analyses are carried out in order to obtain the input ground motion for the building and

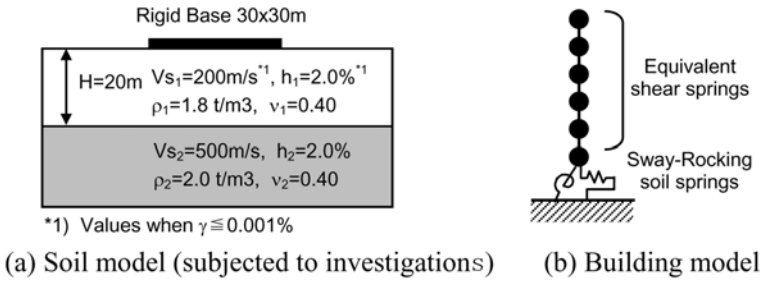

(a) Soil model (subjected to investigations) (b) Building model

Fig. 1 Analysis model

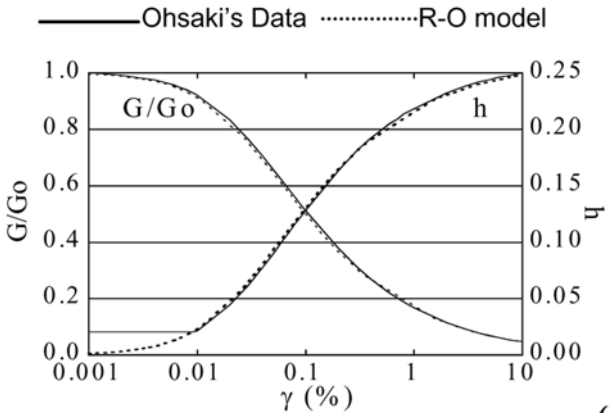

Fig. 2 Nonlinear characteristics of soil

Table 2 Building model data

Story	Height (m)	Weight (t)	Rotational Inertia ($\times 10^5$ tm^2)	Shear stiffness ($\times 10^6$ kN/m)
5	3.0	1080	-	2.369
4	3.0	1080	-	4.264
3	3.0	1080	-	5.685
2	3.0	1080	-	6.632
1	3.0	1080	-	7.106
Basemat	-	1350	5.06	-

the soil's physical properties, which are the basis of the computation of soil impedance. The surface layer is divided into ten elements and the viscous boundary of the physical properties of the base rock is set under the lowest element. Then, 1-dimensional linear and nonlinear analyses are carried out.

El Centro1940 is used for the input ground motion. The analysis time step (ΔT) is set at 0.005sec. The duration and the maximum acceleration are set at 10sec and 300Gal respectively. The wave is defined as double the upward wave (2E) at the top of the base rock (the position of the viscous boundary).

Fig. 3 shows the maximum acceleration distribution of the surface layer as well as the maximum strain distribution obtained from the soil response analyses.

The response waves at the ground surface are used in the next step for the input ground motions to the building. In order to eliminate the high frequency noise, the components of these waves from 10 Hz to 20 Hz are gradually reduced and those beyond 20 Hz are omitted. Fig. 4 compares the response acceleration waves at the ground surface with the input ground motion.

3.3 Soil impedance and impulse response

The soil impedance in each case is computed using the TLEM.

Values for $\gamma = 0.001\%$ are used for Soil-L. As for Soil-NL, the equivalent shear velocity Vs and the damping ratio h at each position of the surface layer are estimated from the G-γ and h-γ

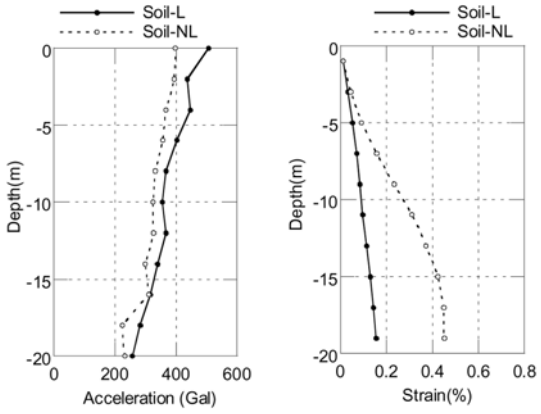

(a) Maximum acceleration (b) Maximum shear strain

Fig. 3 Results of soil response analysis

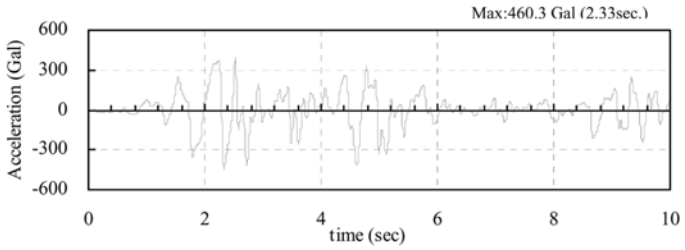

(a) Response wave at ground surface (Soil-L)

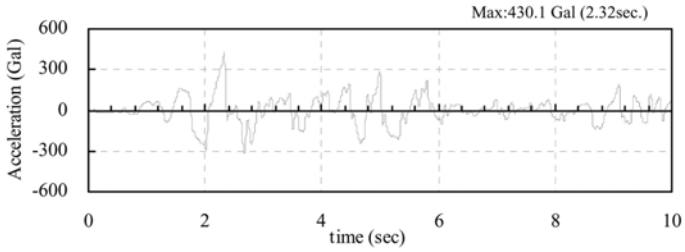

(b) Response wave at ground surface (Soil-NL)

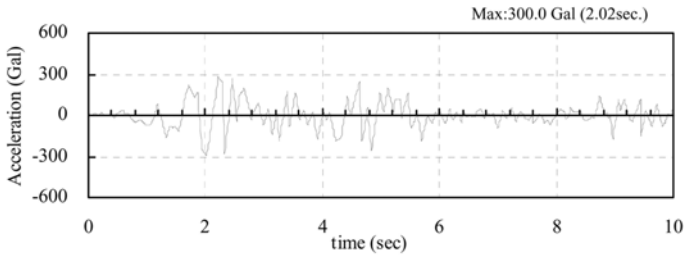

(c) Input wave (Elcentro NS 300Gal)

Fig. 4 Comparison in acceleration wave

Table 3 Maximum strain and corresponding soil properties

GL	Linear			Non-Linear		
	Max Strain (%)	*Vs* (m/s)	*h*	Max Strain (%)	*Vs* (m/s)	*h*
0 ~ -2	0.013	200	0.02	0.011	190.6	0.024
~ -4	0.034			0.044	165.3	0.082
~ -6	0.052			0.092	145.3	0.123
~ -8	0.071			0.157	129.8	0.151
~ -10	0.085			0.233	118.6	0.169
~ -12	0.098			0.310	110.9	0.180
~ -14	0.114			0.373	105.9	0.187
~ -16	0.130			0.424	102.4	0.193
~ -18	0.143			0.449	100.9	0.195
~ -20	0.155			0.453	100.7	0.195

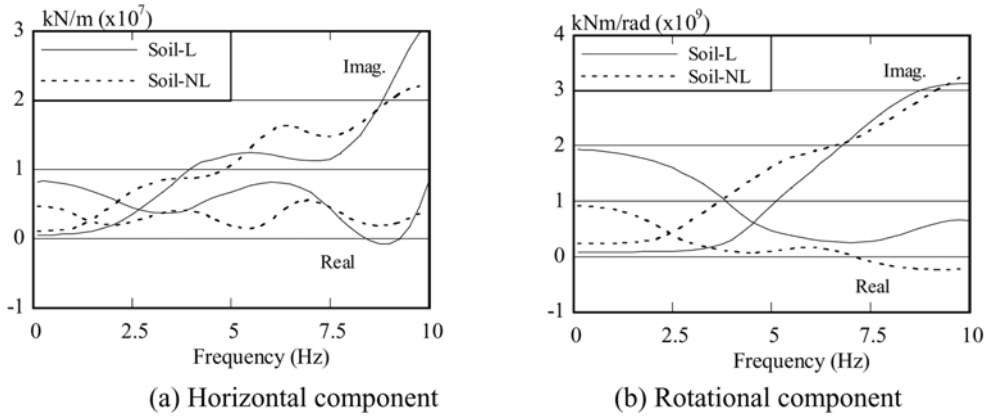

Fig. 5 Calculated soil impedance by TLEM

relationships in Fig. 2 using the maximum strain of each element. The obtained physical properties of the soil for Soil-NL are shown in Table 3.

The soil impedance is computed under the condition that the horizontal component and the rotational component are uncoupled. Fig. 5 shows the soil impedance obtained for each case.

Next, these soil impedances are transformed into the time domain using Method B and Method C described in Chapter 2. Table 4 shows the conditions for the transform.

Figs. 6 and 7 show the impulse responses of the horizontal and rotational component respectively, obtained using Method C. A large difference can be seen in the stiffness term (k_0) of the simultaneous component between Soil-L and Soil-NL. It corresponds to the difference of the static stiffness between both cases. With regard to the horizontal component shown in Fig. 6, a peak can be seen at the time delay 0.2 sec in Soil-L both in the stiffness terms (a) and in the damping terms (b). This time delay corresponds to the time ($2H/Vs_1$) in which the wave that has dissipated from the basemat returns after reflecting off the boundary with the base rock (Nakamura 2005). In Soil-NL, the time delay increases and the peak is reduced than in Soil-L due to the softening of the surface layer and the increase in its damping. In the rotational component shown in Fig. 7, the

Table 4 Transform data for methods B & C

Impedance		Impulse Response		
Number of Data	Frequency of Complex Data (Hz)	Δt (sec)	Simultaneous Components	Time-Delay Components*)
21	0.1, 0.5, 1.0, 1.5, ·· 9.5, 10.0	0.1	k_0, c_0, m_0	$k_1 \sim k_{20}$, $c_1 \sim c_{19}$

*) $k_j = k(j\ \Delta t)$, $c_j = c(j\ \Delta t)$

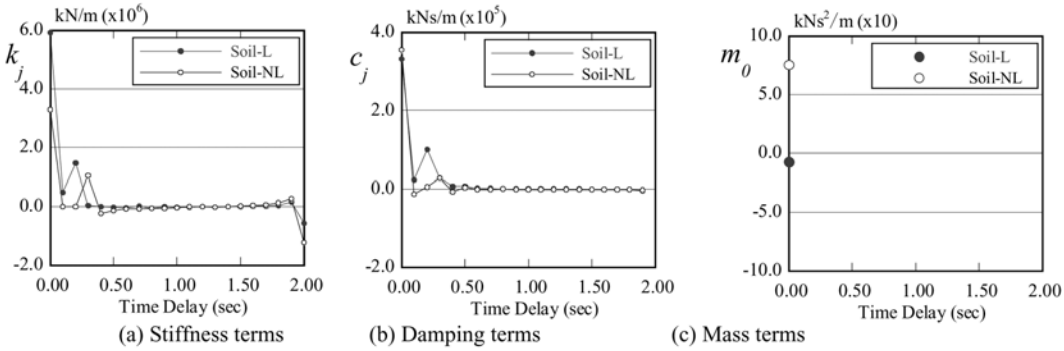

Fig. 6 Impulse response (Horizontal)

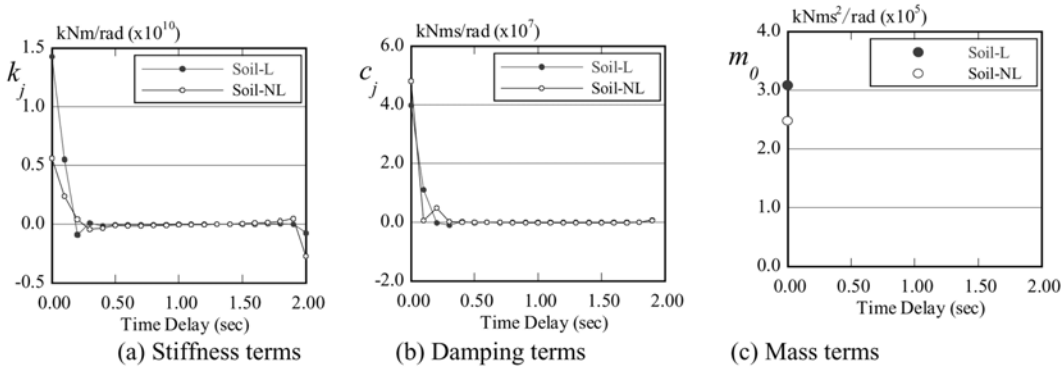

Fig. 7 Impulse response (Rotational)

characteristics of the peak mentioned above are not evident.

In the stiffness terms in Figs. 6 and 7, the stiffness values steeply drop at time delay 2.00 sec. It is considered that this is because the non-causality of the impedance tends to gather into the values in the proposed transform methods. These values cause the fluttering in the recovered impedance in the frequency domain and they cause the inaccuracy of the response in the time domain (Nakamura (2006b)). Then, these terms are omitted because the time delay components only from 0.1 to 0.5 sec are used in the time history analyses in the section 5 and 6.

Tables 5 and 6 compare the simultaneous components (k_0, m_0) obtained from Method B and modified by Method C. In Soil-L, the difference between the two is small, but in Soil-NL there is a great difference. It can be considered that this is because Method B is very accurate in Soil-L due to

Table 5 Modifications of simultaneous components (Horizontal)

Case	k_0 ($\times 10^6$ kN/m)		m_0 (kNs^2/m)	
	Method-B	Method-C	Method-B	Method-C
Linear	6.45	5.93 (0.92)*	-83.7	-7.51 (0.09)
Nonlinear	4.47	3.29 (0.74)	35.0	75.4 (2.15)

*) Number in ( ) of method-C is the ratio to method-B

Table 6 Modifications of simultaneous components (Rotational)

Case	k_0 ($\times 10^9$ kNm/rad)		m_0 ($\times 10^5$ kNms^2/rad)	
	Method-B	Method-C	Method-B	Method-C
Linear	1.51	1.43 (0.92)*	3.16	3.08 (0.97)
Nonlinear	0.83	0.56 (0.67)	2.55	2.48 (0.97)

*) Number in ( ) of method-C is the ratio to method-B

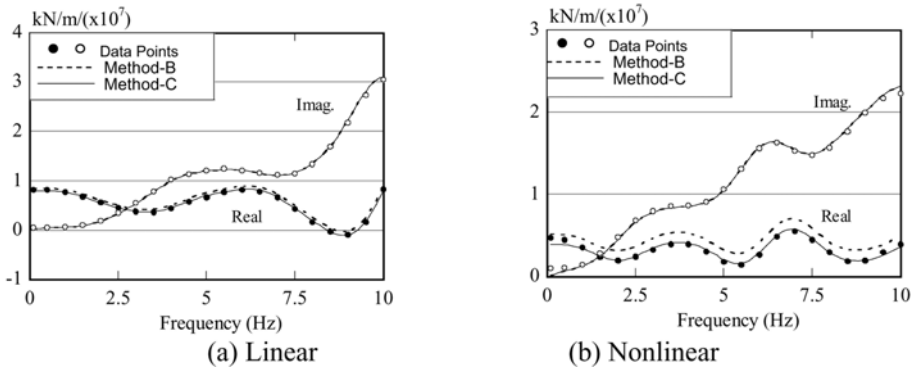

Fig. 8 Recovered impedance (Horizontal)

the small hysteresis damping of the soil and the impedance being almost causal. However, in Soil-NL the effects of Method C are produced due to the increase in the hysteresis damping of the soil and the impedance being noncausal.

The reason why the value for m_0 of the horizontal component obtained using Method B greatly differs from that obtained using Method C is because the negligible absolute value of m_0 is extremely small. Owing to this, with regard to the horizontal component only, the impedance of the soil can be satisfactorily transformed into the time domain using Method A without any consideration of m_0.

Figs. 8 and 9 show the impedance recovered by the obtained impulse response (the simultaneous components (k_0, c_0, m_0) and the first 5 terms of the time delay components ($k_1 \sim k_5$, $c_1 \sim c_5$)). The data from the original impedance is shown in the figure for comparison.

All recovered impedances correspond quite well to the original impedances. In Soil-L, the recovered impedances from both Methods B and C correspond very well to the original data. This is because the damping ratio of the surface layer is small and the original impedance is almost causal.

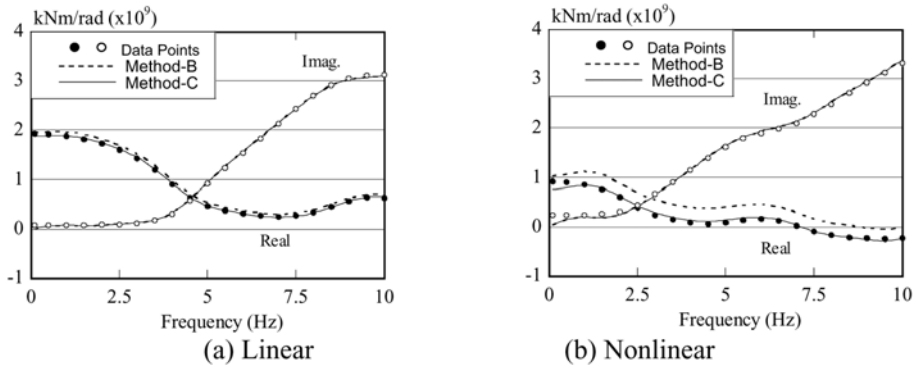

Fig. 9 Recovered impedance (Rotational)

On the other hand, in Soil-NL the recovered impedance using Method B differs from the original data in their real parts because the damping ratio is large and the original impedance is noncausal, but this difference is improved in Method C.

In the range of 0 ~ 0.5 Hz, a few differences can be seen between the data obtained from Methods B ,C and the original data. The difference is caused because the original noncausal function is modified to the causal function.

3.4 Equation of motion

Eq. (12) indicates the equation of motion in the frequency domain for the soil-structure interaction system. Where $u(\omega)$ indicates the response displacement vector at each part and M, C, K indicate the mass, damping and stiffness matrix at each part. The suffices s and b show the above-ground part of the building and its under-ground part. $y_0(\omega)$ and $[I(\omega)]$ indicate the input ground motion and the soil impedance matrix respectively.

Eq. (13) shows the equation of motion of method B or C in the time domain taking into account the frequency dependency of the impedance. Where $u(t)$ and $y_o(t)$ are the displacement vector and the input seismic motion in the time domain, respectively. $[m_0]$, $[c_0]$ and $[k_0]$ are the soil impedance matrices that correspond to the simultaneous components.

$\{R_f(t)\}$ is the force vector determined by the time-delay coefficients and the past displacement and velocity as Eq. (14). n' shows the number of the time delay components which are taken into account.

$$\left(-\omega^2 \cdot \begin{bmatrix} M_s & 0 \\ 0 & M_b \end{bmatrix} + i\omega \cdot \begin{bmatrix} C_{ss} & C_{sb} \\ C_{bs} & C_{bb} \end{bmatrix} + \begin{bmatrix} K_{ss} & K_{sb} \\ K_{bs} & K_{bb} + [I(\omega)] \end{bmatrix}\right) \begin{Bmatrix} u_s(\omega) \\ u_b(\omega) \end{Bmatrix} = -\ddot{y}_0(\omega) \begin{Bmatrix} M_s \\ M_b \end{Bmatrix} \tag{12}$$

$$\begin{bmatrix} M_s & 0 \\ 0 & M_b + [m_0] \end{bmatrix} \begin{Bmatrix} \ddot{u}_s(t) \\ \ddot{u}_b(t) \end{Bmatrix} + \begin{bmatrix} C_{ss} & C_{sb} \\ C_{bs} & C_{bb} + [c_0] \end{bmatrix} \begin{Bmatrix} \dot{u}_s(t) \\ \dot{u}_b(t) \end{Bmatrix} + \begin{bmatrix} K_{ss} & K_{sb} \\ K_{bs} & K_{bb} + [k_0] \end{bmatrix} \begin{Bmatrix} u_s(t) \\ u_b(t) \end{Bmatrix} = -\ddot{y}_0(t) \begin{Bmatrix} M_s \\ M_b \end{Bmatrix} + \begin{Bmatrix} 0 \\ R_f(t) \end{Bmatrix} \tag{13}$$

$$\{R_f(t)\} = -\sum_{j=1}^{n'} \{[c_j] \cdot \dot{u}_b(t - t_j) + [k_j] \cdot u_b(t - t_j)\} \qquad \text{Where } t_j = j \cdot \Delta t, \quad n' \le N - 1 \tag{14}$$

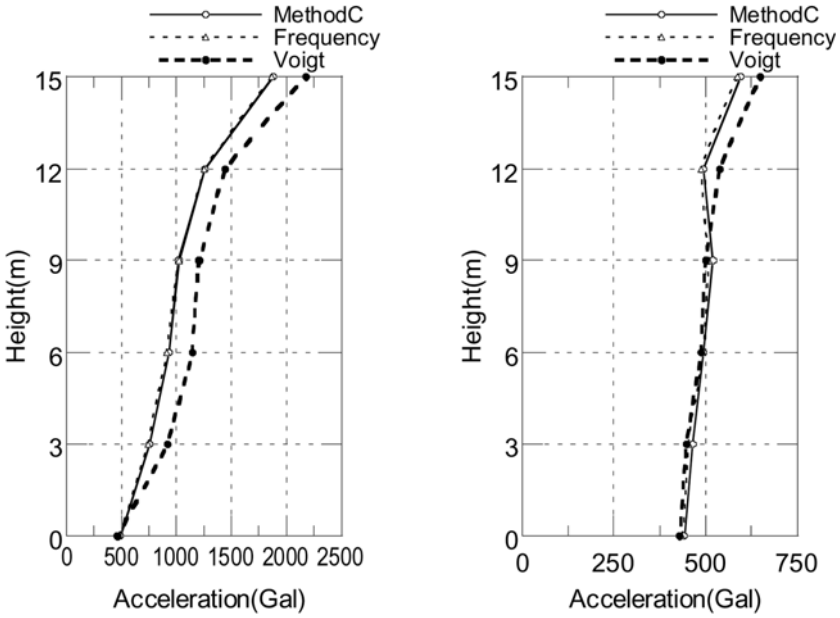

Fig. 10 Comparison of maximum acceleration (Linear building)

3.5 Time history response analysis of building (Linear)

For the purpose of confirming the validity of the proposed transform method to the time domain, the results obtained from the time history seismic analysis carried out using the transformed impulse response are compared with those from the frequency response analysis using the original impedance.

The time history response analysis is carried out using Eq. (13) using the Newmark' β method ($\beta = 1/4$). The soil impedance is estimated using the simultaneous components (k_0, c_0, m_0) and 5 terms for each of the time delay components ($k_1 \sim k_5$ and $c_1 \sim c_5$) by Method C under the condition of $t_j = j\,\Delta t$, $\Delta t = 0.1$sec. It is the same manner as that shown in Fig. 8 and 9. The time step ($\Delta T = 0.005$ sec) for the response analysis does not necessarily agree with the time step (Δt) for the impulse response. In this study (see Nakamura 2006a), the values at intervals of 20 time steps are used for the velocity and the displacement in Eq. (14).

The frequency response analysis is carried out using Eq. (12) in the range of $0 \sim 20$ Hz with the analysis frequency step (Δf) of 0.0977Hz. The soil impedance is a diagonal matrix of 2×2 with an uncoupled horizontal degree of freedom and a rotational degree of freedom.

Figs. 10 and 11 show the maximum response acceleration and the maximum shear force of the buildings in Soil-L and Soil-NL. In both cases, the results of the time history response analysis match those of the frequency response analysis. The differences of the acceleration and the shear force do not exceed 3%.

The thick broken lines in these figures show the results obtained from the conventional method (the Voigt model). In this model, the stiffness and the damping coefficient are set using the simultaneous components (k_0, c_0) only. In this case, the stiffness component (k_0) is set from the

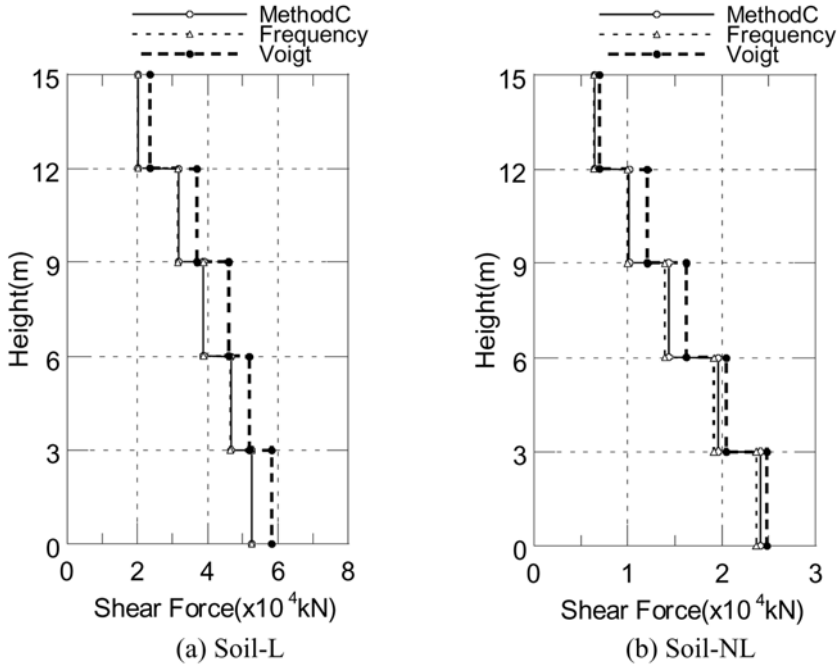

Fig. 11 Comparison of maximum shear force (Linear building)

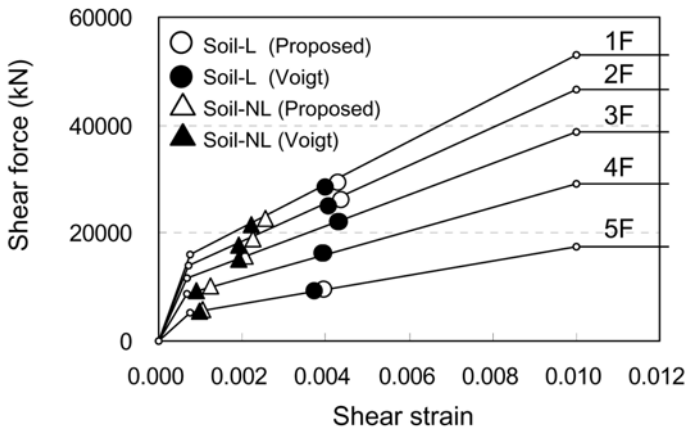

Fig. 12 Skeleton curves of each story of building

static real value and the damping component (c_0) is set based on eigenfrequency of the system (Soil-L: 2.67 Hz, Soil-NL: 2.22 Hz). From these figures, fairly large differences are seen between the results from the Voigt model and the frequency analysis.

From above, it is confirmed that the accuracy of the time history response analyses using the impulse response obtained from the proposed transform methods is high for noncausal problems as well as for causal problems, while the accuracy of the conventional Voigt model is not good.

3.6 Time history response analysis of building (Nonlinear)

In order to confirm the efficiency of the proposed methods, the analysis considering nonlinear building properties is carried out between the proposed methods and the Voigt model in Soil-L and Soil-NL.

The skeleton curves, which show the nonlinear relationships between the shear force and the shear strain, for each story of the building are shown in Fig. 12. The normal tri-linear model is used for the hysteresis curve. The other analysis conditions are the same as those in the previous section.

The maximum responses in each case are plotted in Fig. 12. The nonlinear level of each story is not so strong in these analyses.

Figs. 13 and 14 show the maximum acceleration and the maximum shear force of the buildings. It can be seen that the results of the Voigt model are different from those of the proposed methods in the nonlinear analysis. The differences between the proposed methods and the Voigt model seem to be smaller than those in the linear analysis. It is considered that the effects of the frequency dependency of the soil on the building response reduce according to the increase in the nonlinear level of the building. However, the effects of the frequency dependency of the soil are not small in Soil-NL because the maximum difference in the acceleration is 18% and that in the shear force is 8%.

The computational time for the calculation of the nonlinear analyses using the proposed methods is around 1 second when using a standard personal computer for these cases Therefore, it can be said that the computational burden for these analyses is small.

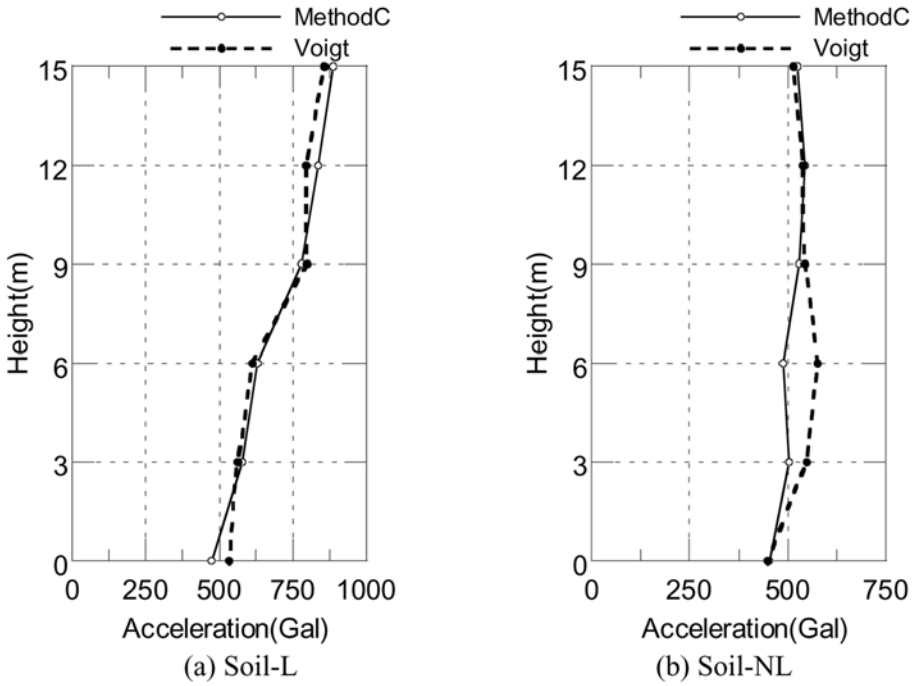

Fig. 13 Comparison of maximum acceleration (Nonlinear building)

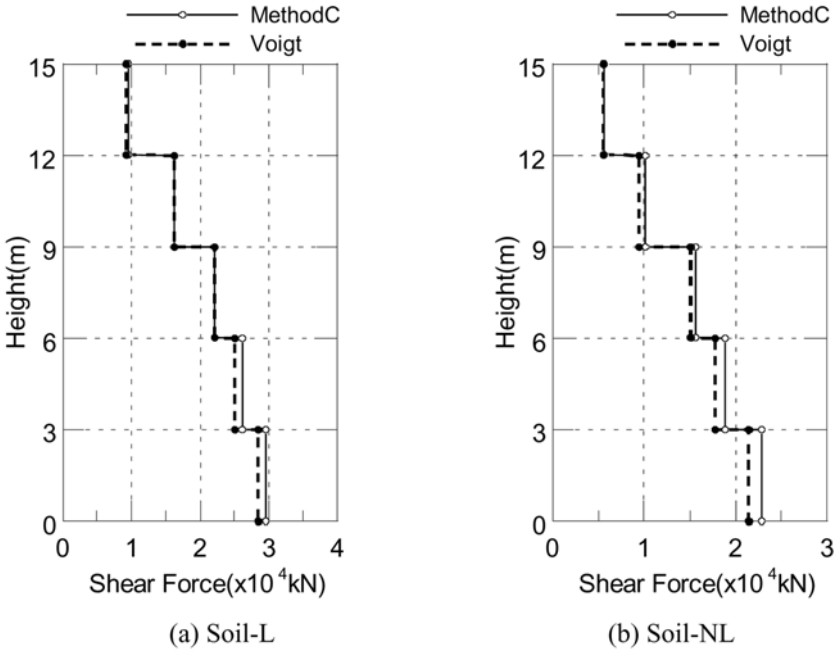

Fig. 14 Comparison of maximum shear force (Nonlinear building)

4. Conclusions

In order to estimate the seismic behavior of buildings, it is important to accurately transform the soil impedance in the frequency domain to the impulse response in the time domain to consider both nonlinear characteristics of the buildings and the frequency dependency of the soil impedance.

In this paper, some practical transform methods and seismic response analyses considering frequency dependent soil impedance in the time domain using the impulse response obtained by the transform were shown.

First, the formulation of the proposed transform methods was explained. The soil impedances of 2-layered soil were computed using the TLEM and these soil impedances were transformed into the time domain using the proposed methods.

Next, the earthquake response analyses of the structure on 2-layered soil were carried out in the time domain in order to study the characteristics of the proposed methods.

By comparing these response results with the frequency response analysis results, it was confirmed that the results obtained from the proposed methods are more accurate than those from the conventional Voigt model. Moreover, it was shown that the proposed method is efficient for the nonlinear analysis carried out in a little computational time.

As a result, the validity and efficiency of the proposed methods were confirmed.

References

de Barros, F.C.P. and Luco, J.E. (1990), "Discrete models for vertical vibrations of surface and embedded foundations", *Earthq. Eng. Struct. Dyn.*, **19**, 289-303.

Hayashi, Y. and Katsukura, Y. (1990), "Effective time domain soil-structure interaction analysis based on FFT algorithm with causality condition", *Earthq. Struct. Dyn.*, **19**, 693-708.
Meek, J.W. (1990), "Recursive analysis of dynamic phenomena in civil engineering", *Bautechnik*, **67**, 205-210 (In German).
Motosaka, M. and Nagano, M. (1992), "Recursive evaluation of convolution integral in nonlinear soil-structure interaction analysis and its applications", *J. Struct. Constr. Eng. (AIJ)*, **436**, 71-80 (In Japanese).
Nakamura, N. (2005), "A practical method for estimating dynamic soil stiffness on surface of multi-layered soil", *Earthq. Eng. Struct. Dyn.*, **34**, 1391-1406.
Nakamura, N. (2006a), "A practical method to transform frequency dependent impedance to time domain", *Earthq. Eng. Struct. Dyn.*, **35**, 217-231.
Nakamura, N. (2006b), "Improved methods to transform frequency dependent dynamic stiffness to time domain", *Earthq. Eng. Struct. Dyn.*, **35**, 1037-1050.
Ohsaki, Y., Hara, A. and Kiyota, Y. (1978), "Stress-strain model of soils for seismic analisys", *Proc of 5th Japan Earthquake Eng. Symposium*, 697-704 (in Japanese).
Tajimi, H., (1980), "A contribution to theoretical prediction of dynamic stiffness of surface foundations", *Proceeding of 7th World Conference on Earthquake Engineering, Istanbul, Turkey*, 105-112.
Wolf, J.P. and Obernhuber, P. (1985), "Nonlinear soil-structure interaction analysis using dynamic stiffness or flexibility of soil in the time domain", *Earthq. Eng. Struct. Dyn.*, **13**, 195-212.
Wolf, J.P. and Motosaka, M. (1989), "Recursive evaluation of interaction force of unbounded soil in the time domain", *Earthq. Struct. Dyn.*, **18**, 345-363.
Wolf, J.P. (1997), "Spring-dashpot-mass models for foundation vibrations", *Earthq. Eng. Struct. Dyn.*, **26**, 931-949.
Wu, W.H. and Lee, W.H. (2002), "Systematic lumped-parameter models for foundations based on polynomial-fraction approximation", *Earthq. Eng. Struct. Dyn.*, **31**, 1383-1412.